XLI CILAMCE
XLI Ibero-Latin American Congress on Computational Methods in Engineering
16-19 November, 2020 FOZ DO IGUAÇU PARANÁ - BRAZIL

Buckling and vibration of slender rings and pipes on an elastic foundation

Mariana Barros dos Santos Dias[1], Paulo B. Gonçalves[1]

[1]*Dept. of Civil and Environmental Engineering, Pontifical Catholic University of Rio de Janeiro*
Gávea, 22451-900, RJ, Brasil
marianabsantosdias@gmail.com, paulo@puc-rio.br

Abstract. It is well known that thin-walled elastic rings and pipes are prone to buckling instabilities when under external pressure. A particularly interesting example is the buckling of a thin, elastic ring under hydrostatic pressure. The buckling load is strongly influenced by the follower force nature of the pressure and, if this effect is neglected, the prediction of the critical buckling load can be as much as 50% for very thin rings. This work studies, using a variational nonlinear formulation, the buckling and vibration characteristics of rings and pipes resting on an elastic Pasternak foundation. First the equation of motion of the pre-loaded ring is derived and the analytical solution of the eigenvalue problems are obtained. The parametric analysis shows the influence of the geometric and physical parameters on the critical load, natural frequencies and load-frequency nonlinear relation, considering the follower force effect of the hydrostatic pressure.

Keywords: Structural stability, critical load, vibration frequencies, elastic foundation, Pasternak foundation.

1 Introduction

Rings and pipes have a wide range of applications in civil, mechanical and biomechanical engineering and in many applications they are surrounded by an elastic medium. This work studies, using a variational nonlinear formulation [1, 2], the buckling and vibration characteristics of rings and pipes resting on an elastic Pasternak foundation [3, 4]. For a long free pipe, the buckling equation can be derived using the Euler buckling theory, by modelling the pipe as a ring [2]. The stability and vibration analysis of rings and long cylindrical shells continues to be an important research subject due to various technological applications with recent contributions including [5, 6, 7]. The parametric analysis shows the influence of the geometric and physical parameters on the critical load, natural frequencies and load-frequency nonlinear relation, considering the follower force effect of the hydrostatic pressure.

2 Formulation

Consider a circular ring of radius a, rectangular cross-section with base b and thickness h, under hydrostatic pressure of magnitude q, as illustrated in Figure 1, where r and θ are the radial and circumferential coordinates. The ring material is isotropic, homogeneous, elastic and linear with Young modulus E and mass per unit volume ρ. The total potential energy of a ring under hydrostatic pressure is given by [1]:

$$\Pi = \int_0^{2\pi} \left\{ \frac{EAa}{2}\left[\frac{v'+w}{r} + \frac{1}{2}\left(\frac{v-w'}{r}\right)^2\right]^2 + \frac{EIa}{2}\left(\frac{v'-w''}{a^2}\right)^2 \right\} d\theta + qa\int_0^{2\pi}\left[w + \frac{1}{2a}\left(v^2 - vw' + v'w + w^2\right)\right] d\theta \quad (1)$$

where A and I are respectively the area and moment of inertia of the cross section, w and v are the radial and circumferential displacements, respectively, and $(\ )' = \partial/\partial\theta$.

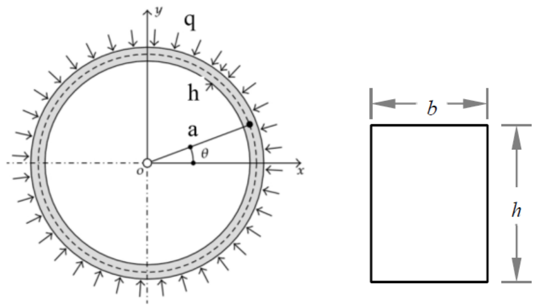

Figure 1. Ring under hydrostatic pressure: geometry and coordinate system

The potential energy of the Pasternak foundation takes the form [3, 4]:

$$U_f = \frac{1}{2}K_r \int_0^{2\pi} w^2 a \; d\theta \; + \frac{1}{2}K_g \int_0^{2\pi} \frac{w_{,\theta}^2}{a} d\theta \tag{2}$$

where the reaction of the foundation is determined by a radial spring constant K_r (the modulus of subgrade reaction in the Winkler foundation, which represents compressive soil resistance) in combination with a parameter K_g, which can account for the actual shearing effect of soils.

The kinetic energy of the slender ring with mass density ρ considering rotatory inertia is given by

$$T = \frac{1}{2}A\rho a \int (\dot{v}^2 + \dot{w}^2)\, d\theta + \frac{1}{2}I\rho a \int \left(\frac{\dot{v}-\dot{w}'}{a}\right)^2 d\theta \tag{3}$$

where the dot represents the partial derivative with respect to time ($\partial/\partial t$).

The analytical solution of the buckling and vibration modes takes the form:

$$v = B\,\mathrm{sen}(n\theta), \;\; w = C\cos(n\theta)\,, \tag{4}$$

where n is the circumferential wavenumber.

Based on (4), the stiffness matrix, K_E, and the geometric matrix, K_G, are given respectively by:

$$K_E = \begin{bmatrix} En^2(I + Aa^2) & En(In^2 + Aa^2) \\ En^2(In^2 + Aa^2) & E(In^4 + Aa^2) + a^2\left(K_r a^2 + K_g n^2\right) \end{bmatrix}, \quad K_G = \begin{vmatrix} 0 & 0 \\ 0 & -a^3(n^2-1) \end{vmatrix} \tag{5}$$

while the mass matrix takes the form:

$$M = -\rho a^2 \begin{bmatrix} I + Aa^2 & In \\ In & In^2 + Aa^2 \end{bmatrix} \tag{6}$$

The characteristic equation $|K_E - qK_G| = 0$ of the stability eigenvalue problem leads to the following sequence of eigenvalues:

$$\bar{q}_n = \left\{\left[n^2(n^2-2\,) + 1 + \bar{K}_r + \bar{K}_g n^2\right]/(n^2-1)\right\} \qquad n = 2,3,4\,... \tag{7}$$

where the following nondimensional quantities are used: $\bar{q} = qa^3/EI$; $\bar{K}_r = K_r a^4/EI$; $\bar{K}_g = K_g a^2/EI$. For a long pipe the stiffness is rewritten as $EI = Eh^3/12(1-\upsilon^2)$ where υ is the Poisson ratio [2].

The characteristic equation $|(K_E - qK_G) - \omega^2 M| = 0$ of the undamped free vibration eigenvalue problem leads to the following eigenvalues for the flexural natural frequencies of the loaded ring:

$$\bar{\omega}_1 = \left\{\frac{1}{2\delta(n^2+\delta+1)}\left\{\delta(2n^4-n^2+1)+\delta^2(n^2+1)-\bar{q}(\delta+1)(n^2-1)+(\delta+1)\left(\bar{K}_r+\bar{K}_g n^2\right)-\left\{\delta^4(n^4+2n^2+1)+2\delta^3(5n^4-2n^2+1)+\delta^2(9n^4-6n^2+1)+[2\delta\bar{q}(\bar{q}+\delta^2)+\bar{q}^2(1+\delta^2)](n^4-2n^2+1)+4\delta^2\bar{q}(2n^4-3n^2+1)+2\delta\bar{q}(3n^4-4n^2+1)-[2\delta^2(\bar{q}+\delta)+2\bar{q}(1+2\delta)](n^2-1)\left(\bar{K}_r+\bar{K}_g n^2\right)-4\delta^2(2n^2-1)\left(\bar{K}_r+\bar{K}_g n^2\right)-2\delta(3n^2-1)\left(\bar{K}_r+\bar{K}_g n^2\right)+(\delta^2+2\delta+1)\left(\bar{K}_r+\bar{K}_g n^2\right)^2\right\}^{1/2}\right\}\right\}^{1/2} \quad (8)$$

where $\delta = 12(h/a)^2$, $\bar{\omega} = \sqrt{\rho a^2\omega^2/E}$ in the nondimensional frequency and ω is the frequency in rad/s corresponding to flexural mode. The higher second eigenvalue $\bar{\omega}_2$ corresponds to circumferential motions.

3 Results

Using the deduced nondimensional analytical expressions a detailed parametric analysis is now conducted to study the effect of the foundation on the critical load, natural frequencies and on the load-frequency relation.

3.1 Critical load

Figure 2(a) shows the variation of the critical loads as a function of the circumferential wavenumber n for selected values of the Winkler foundation stiffness parameter $\bar{K}_r$. For $\bar{K}_r = 0$, the critical load corresponds to $n = 2$ with $\bar{q}_{cr} = 3$ [1, 2]. If the follower force effect of the hydrostatic pressure in not considered in Eq. (1) $\bar{q}_{cr}$ increases to 4.5. As $\bar{K}_r$ increases, the critical load and the number of circumferential waves associated with the critical load increases. Figure 2(b) shows the variation of the critical loads as a function of foundation stiffness $\bar{K}_r$, where the variation of the critical wavenumber n with the foundation stiffness is clearly observed.

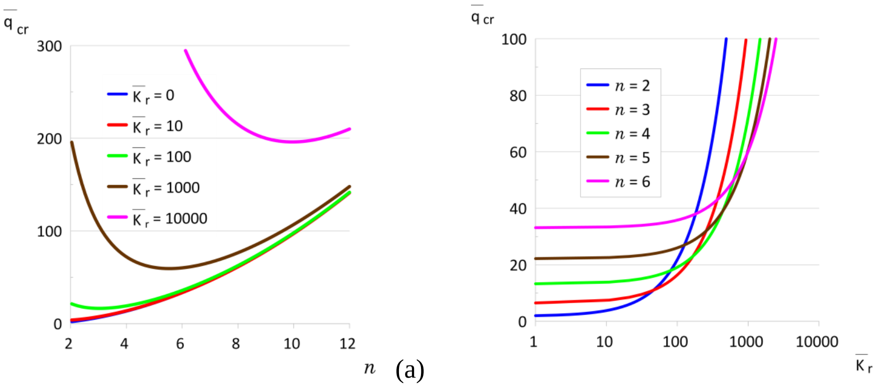

Figure 2. Variation of the critical load (a) with the number of circumferential waves n for selected values of the foundation stiffness $\bar{K}_r$; (b) with the foundation stiffness $\bar{K}_r$ for selected values of n.

Figure 3 illustrates the influence of the foundation stiffness parameter $\bar{K}_g$ on the critical load. As observed in Eq. (7), the load increases with $\bar{K}_g$ and n^2.

Schmidt [8] discusses the different expressions and values of the critical pressure of slender rings as a function of the load modeling and shows that generally $\bar{q}_{cr} = k^2$ with k^2 varying between 0.701 and 5.6, illustrating the importance of the load description on the results.

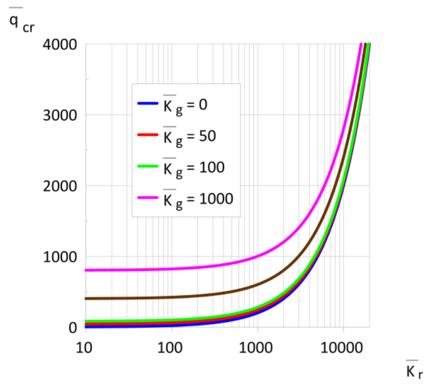

Figure 3. Variation of the critical load with the foundation stiffness $\bar{K}_r$ for selected values of the Pasternak foundation stiffness parameter $\bar{K}_g$ and $n = 2$

3.2 Natural Frequencies

Figure 4 shows the variation of the nondimensional frequency parameter $\bar{\omega}_1$ with n for $a/h = 20$ and selected values of $\bar{K}_r$ considering or not the effect of rotatory inertia. The frequencies increase with n and $\bar{K}_r$, with the fundamental frequency corresponding to $n = 2$. The influence of $\bar{K}_r$ is particularly important for low values of n. The effect of rotatory inertial in negligible even for this value of radius-to-thickness ratio, a/h.

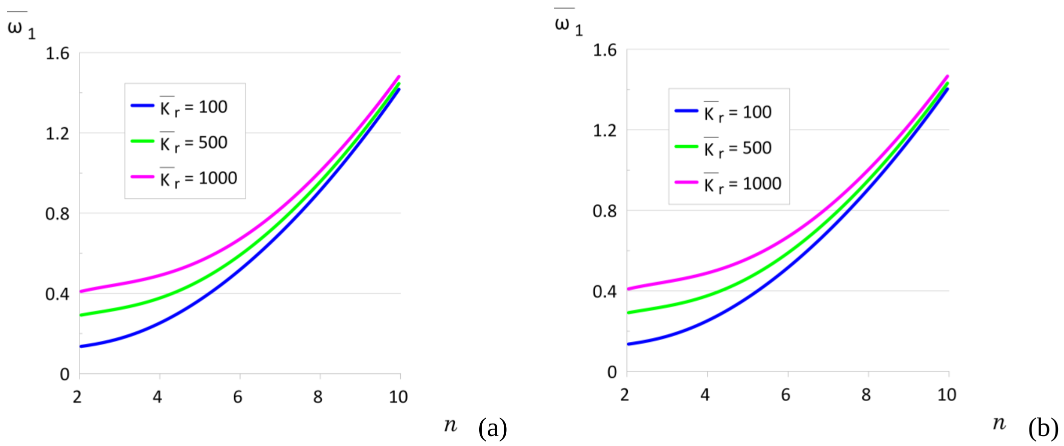

Figure 4. Variation of $\bar{\omega}_1$ with n for $a/h = 20$ and selected values of $\bar{K}_r$ (a) disregarding the effect of rotatory inertia, (b) considering the effect of rotatory inertia

Figure 5 illustrates the influence of the Winkler foundation parameter $\bar{K}_r$ on the four lowest natural frequencies, where in accordance with Figure 4, the flexural natural frequencies increases with n. Initially the influence of the foundation stiffness is very small but for $\bar{K}_r > 10^6$ the natural frequencies increases steadly with $\bar{K}_r$. The difference between the consecutive natural frequencies also increases.

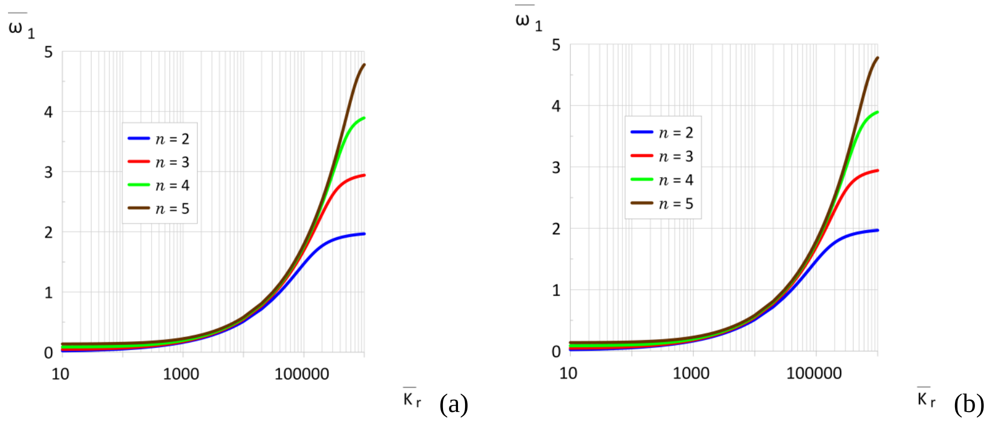

Figure 5. Variation of the four lowest natural frequencies of the ring $\bar{\omega}_1$ as a function of $\bar{K}_r$ (a) disregarding the effect of rotatory inertia (b) considering the effect of rotatory inertia

Figure 6 illustrates the influence of the Pasternak foundation parameters $\bar{K}_r$ and $\bar{K}_g$ on the lowest natural frequencies ($n = 2$). The fundamental frequency increases with $\bar{K}_g$ for a given value of $\bar{K}_r$, being its influence particularly important for $\bar{K}_r < 10^6$. The influence of $\bar{K}_g$ decreases as $\bar{K}_r$ increases and disappears for large values of $\bar{K}_r$ (rigid foundation).

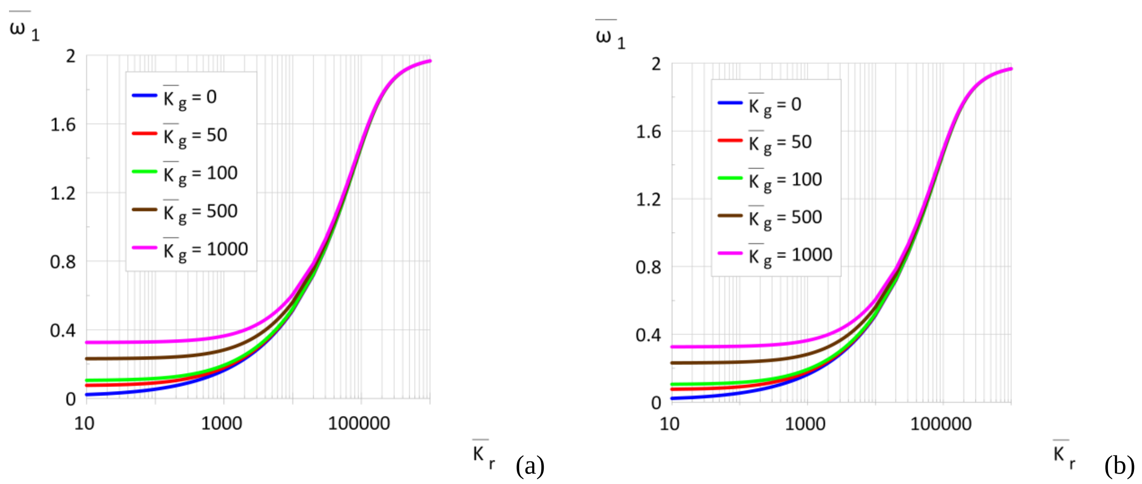

Figure 6. Variation of the lowest natural frequencies of the ring ($n = 2$) as a function of $\bar{K}_r$ for selected values of $\bar{K}_g$, (a) disregarding the effect of rotatory inertia (b) considering the effect of rotatory inertia.

3.3 Load-frequency relation

It is known that in structures liable to buckling the compressive stresses have a strong influence on the natural frequencies with the lowest natural frequency becoming zero at the critical load. Figure 7 shows the variation of the four lowest natural frequencies of the ring with the foundation stiffness $\bar{K}_r = 100$ and $a/h = 50$ with the applied pressure $\bar{q}$. For the unloaded ring the frequencies increase with the circumferential wavenumber n, but, as $\bar{q}$ increases there is a change in the sequence of vibration modes, and the lowest natural frequency becomes associated with $n = 3$, since for the adopted value of $\bar{K}_r$ this is the number of waves of the critical mode.

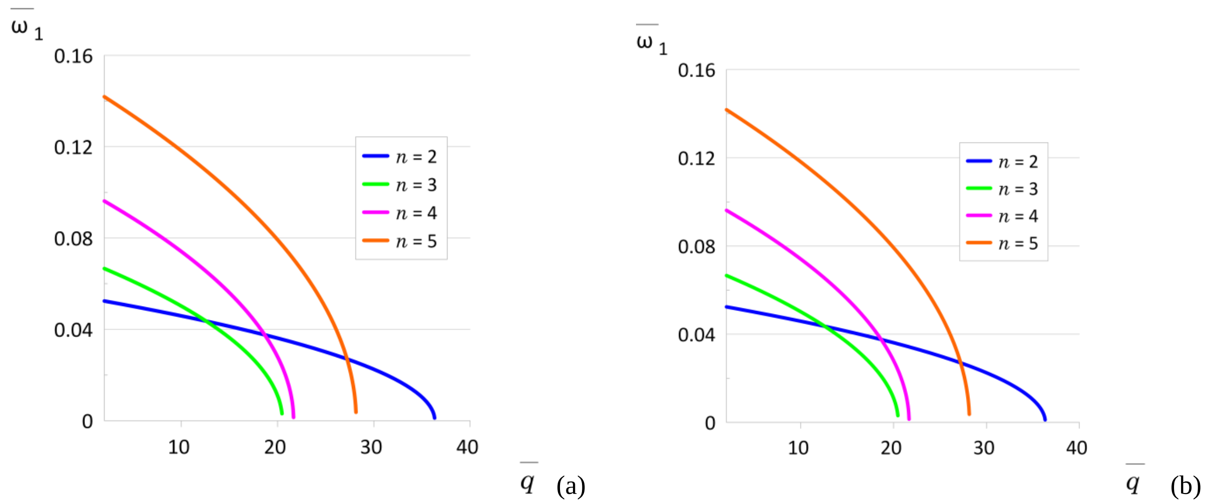

Figure 7. Variation of the four lowest natural frequencies of the ring with the applied pressure $\bar{q}$ (a) disregarding the effect of rotatory inertia (b) considering the effect of rotatory inertia. stiffness $\overline{K}_r = 100$ and $a/h = 50$.

Thus the sequence of vibration modes in loaded rings changes with the applied load and the foundation stiffness parameters. As a consequence, for certain parameter values there is a coincidence of natural frequencies leading to possible internal resonances.

4 Conclusions

The variational formulation for the dynamic response of a ring or long cylindrical shell (pipe) under hydrostatic pressure resting on Pasternak foundation is presented in this study and closed-form solutions are derived for the critical load, natural frequencies and frequency-load relation. The results of a detailed parametric analysis show the influence of the applied load and of the two stiffness parameters of the Pasternak foundation on the buckling and vibration characteristics of the ring. The Pasternak foundation forms an attractive alternative to the Winkler foundation regarding the larger flexibility of the simple 2-parameter model.

Acknowledgements. The authors acknowledge the financial support of the Brazilian research agencies CAPES [finance code 001], CNPq and FAPERJ-CNE.

Authorship statement. The authors hereby confirm that they are the sole liable persons responsible for the authorship of this work, and that all material that has been herein included as part of the present paper is either the property (and authorship) of the authors, or has the permission of the owners to be included here.

References

[1] D. O. Brush and B. O. Almroth. *Buckling of bars, plates, and shells*. McGraw-Hill, New York, 1975.
[2] S. Kyriakides and E. Corona. *Mechanics of offshore pipelines: volume 1 buckling and collapse (Vol. 1)*. Elsevier, 2007.
[3] D. N. Paliwal and V. Bhalla. (1993). Large amplitude free vibrations of cylindrical shell on Pasternak foundations. *International journal of pressure vessels and piping*, 54(3), 387-398, 1993
[4] N. D. Duc and P. T. Thang. (2014). Nonlinear response of imperfect eccentrically stiffened ceramic–metal–ceramic FGM thin circular cylindrical shells surrounded on elastic foundations and subjected to axial compression. *Composite Structures*, 110, 200-206, 2014.
[5] J. Gumbel. New approach to design of circular liner pipe to resist external hydrostatic pressure. *In: Pipelines 2001: Advances in Pipelines Engineering and Construction*. p. 1-18, 2001
[6] H. Showkati and R. Shahandeh. Experiments on the buckling behavior of ring-stiffened pipelines under hydrostatic pressure. *ASCE Journal of engineering mechanics*, v. 136, n. 4, p. 464-471, 2010.
[7] E. Azzuni and S. Guzey. A perturbation approach on buckling and postbuckling of circular rings under nonuniform loads. *International Journal of Mechanical Sciences*, v. 137, p. 86-95, 2018.
[8] R. Schmidt. Critical constant-directional pressure on circular rings and hingeless arches. *Zeitschrift für angewandte Mathematik und Physik ZAMP*, 31(6), p. 776-779, 1980.